Article:

Dhimish, Mahmoud, Holmes, Violeta, Mehrdadi, Bruce et al. (1 more author) (2018) Comparing Mamdani Sugeno Fuzzy Logic and RBF ANN Network for PV Fault Detection. Renewable Energy. pp. 257-274. ISSN 0960-1481

https://doi.org/10.1016/j.renene.2017.10.066

Comparing Mamdani Sugeno Fuzzy Logic and RBF ANN Network for PV Fault Detection

Mahmoud Dhimish, Violeta Holmes, Bruce Mehrdadi, Mark Dales

School of Computing and Engineering, University of Huddersfield, United Kingdom

---

Abstract

This work proposes a new fault detection algorithm for photovoltaic (PV) systems based on artificial neural networks (ANN) and fuzzy logic system interface. There are few instances of machine learning techniques deployed in fault detection algorithms in PV systems, therefore, the main focus of this paper is to create a system capable to detect possible faults in PV systems using radial basis function (RBF) ANN network and both Mamdani, Sugeno fuzzy logic systems interface.

The obtained results indicate that the fault detection algorithm can detect and locate accurately different types of faults such as, faulty PV module, two faulty PV modules and partial shading conditions affecting the PV system. In order to achieve high rate of detection accuracy, four various ANN networks have been tested. The maximum detection accuracy is equal to 92.1%. Furthermore, both examined fuzzy logic systems show approximately the same output during the experiments. However, there are slightly difference in developing each type of the fuzzy systems such as the output membership functions and the rules applied for detecting the type of the fault occurring in the PV plant.

Keywords: Photovoltaic System, Photovoltaic Faults, Fault Detection, ANN Networks, Fuzzy Logic Systems

---

1. INTRODUCTION

The monitoring and regular performance supervision on the functioning of grid-connected photovoltaic (GCPV) systems is necessary to ensure an optimal energy harvesting and reliable power production. The development of diagnostic methods for fault detection in the PV systems behaviour is particularly important due to the expansion degree of GCPV systems nowadays and the need to optimize their reliability and performance.

There are existing techniques which were developed for possible fault detection in grid-connected PV systems. Some of these techniques use meteorological and satellite data for predicting the faults in the GCPV plants [1 & 2]. However, some of the PV fault detecting algorithms do not require any climate data (solar irradiance and module temperature) such as the earth capacitance measurements established by Taka-Shima [3].

Other PV fault detection algorithms is based on the comparison of simulated and measured yield by analysing the losses of the DC side of the GCPV plant [4-6]. Furthermore, a fault detection method based on the ratio of DC side and the AC side of the PV system is proposed by W. Chine et al [7]. The method can detect five different faults such as faulty modules in a PV string, faulty DC/AC inverter and faulty maximum power point tracking (MPPT) units. On the other hand, S. Silvestre et al [8] proposed a new procedure for fault detection in GCPV systems based on the evaluation of the current and the voltage indicators. The main advantage of this algorithm is to reduce the number of monitoring sensors in the PV plants and integrating a fault detection algorithm into an inverter without using simulation software or additional external hardware devices.

Further fault detection algorithms focus on faults occurring in the AC-side of GCPV systems, as proposed by M. Dhimish et al [9]. The approach uses mathematical analysis technique for identifying faulty conditions in the DC/AC inverter units. Moreover, hot-spot detection in PV substrings using the AC parameters characterization was developed by [10]. The hot-spot detection method can be further used and integrated with DC/DC power converters that operates at the subpanel level. A comprehensive review of the faults, trends and challenges of the grid-connected PV systems is shown in [11-13].

Other PV fault detection approaches use statistical analysis techniques for identifying micro cracks and their impact of the PV output power as presented by [14]. However, T. Zhao at al [15] developed a decision tree (DT) technique for examining two different types of fault using an over-current protection device (OVPD). The first type of fault is the line-to-line that occurs under low irradiance conditions, and the second is line-to-line faults occurring in PV arrays equipped with blocking diodes.

PV systems reliability improvement by real-time field programmable gate array (FPGA) based on switch failures diagnosis and fault tolerant DC-DC converters is presented by [16]. B. Chong [17] suggested a controller design for integrated PV converter modules under partial shading conditions. The developed approach is based on a novel model-based, two-loop control scheme for a particular MIPC system, where bidirectional Cuk DC-DC converters are used as the bypass converters and a terminal Cuk boost functioning as a while system power conditioner.

Nowadays, fuzzy logic systems widely used with GCPV plants. R. Boukenoui et al [18] proposed a new intelligent MPPT method for standalone PV system operating under fast transient variations based on fuzzy logic controller (FLC) with scanning and storing algorithm. Furthermore, [19] presents an adaptive FLC design technique for PV inverters using differential search algorithm. Furthermore, N. Sa-ngawong & I. Ngamroo [20] proposed an intelligent PV farms for robust frequency stabilization in multi-area interconnected power systems using Sugeno fuzzy logic control, similar approach was developed by [21] for power optimization in standalone PV systems.

In [22 & 23] authors have used a Mamdani fuzzy logic classification system which consists of two inputs, the voltage and power ratio, and one output membership function. The results can accurately detect several faults in the PV system such as partial shading and short circuited PV modules.

Artificial intelligent networks (ANN) is another machine leaning technique nowadays is used for detecting faults in PV systems. A learning method based on expert systems is developed by [24] to identify two types of fault (due to the shading effect and to the inverter's failure). Whereas [25] proposed an ANN network that detects faults in the DC side of PV systems which includes faulty bypass diodes and faulty PV modules in a PV string.

A. Millit et al [26] shows that ANN networks is a possible solution for modelling and estimating the output power of a GCPV systems. However, a failure mode prediction and energy harvesting of PV plants to assist dynamic maintenance tasks using ANN based models is proposed by F. Polo et al [27]. Further investigation on a very short term load forecasting for a distribution system with high PV penetration is suggested by S. Sepasi [28]. Finally, B. Amrouche & X. Pivert [30] offered an ANN network based daily local forecasting for global solar radiation (GHI). The ANN model is developed to predict the local GHI based on a daily weather forecast provided by the US National Oceanic and Atmospheric Administration (NOAA) for four neighbouring locations.

The main contribution of this work is to present a new algorithm for isolation and identification of the faults accruing in a PV system. The algorithm is capable to detect several faults such as faulty PV module in a PV string, faulty PV string, faulty MPPT, and partial shading conditions effects the PV system. The proposed algorithm is comparing between two different approaches for detecting failure conditions which can be described as the following:

1. Artificial Neural Network (ANN) Approach:
   Four different ANN networks have been compared using a logged data of several faulty conditions affecting the examined PV plant. The maximum PV fault detection accuracy achieved by the ANN networks is equal to 92.1%.

2. Fuzzy Logic Fault Classification Approach:
   This approach consists of two types of fuzzy logic interface systems: Mamdani and Sugeno. Both fuzzy interface systems were briefly compared and developed using MATLAB/Simulink software. This approach was tested using a faulty PV data which was logged from the examined 1.1 kWp PV plant installed at the University of Huddersfield.

The overall system design is shown in Fig. 1. The PV plant has a capacity of 1.1 kWp. A computer interface has two options, a PV fault detection algorithms which use MATLAB/Simulink software which contains the ANN and the fuzzy logic interface system. Furthermore, LabVIEW software is used for the real-time long-term data monitoring as well as, data logging software environment.

This paper is organized as follows: Section 2 presents the data acquisition in the PV plant. Section 3 describes the methodology used, Fault detection algorithm and diagnosis rules are presented, while section 4 lists the results and discussion of the work. Finally, section 5 describes the conclusion and future work.

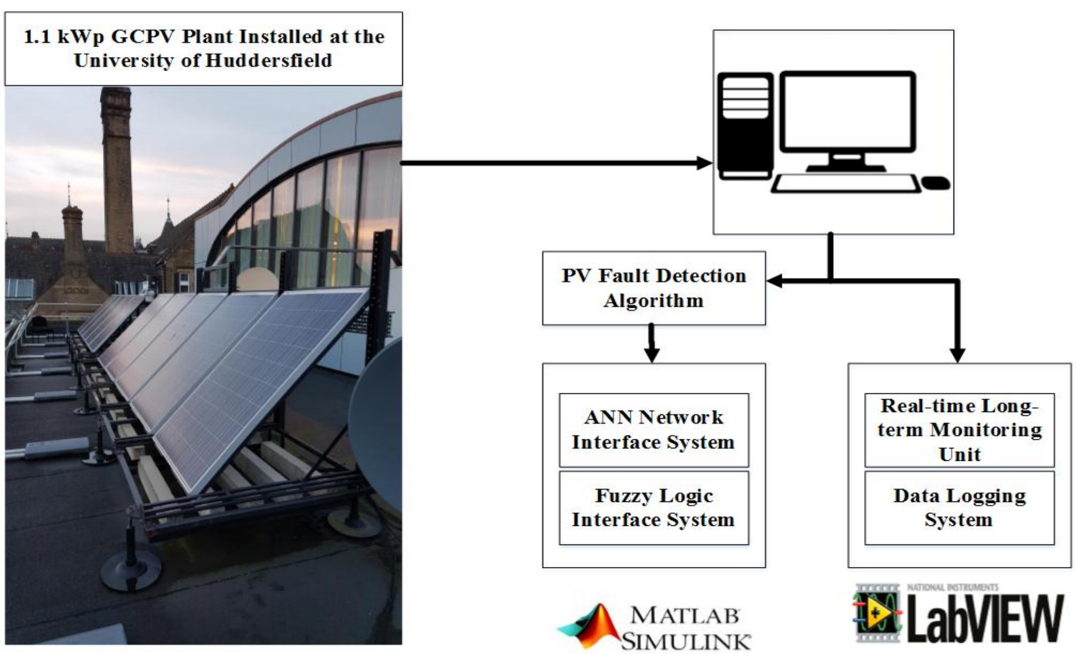

Fig. 1. Overall System Architecture Design for the Examined PV Plant

2. *Faults in Photovoltaic Plants*

The faults occurring in a PV system are mainly related to the PV array, MPPT units, DC/AC inverters, the storage system and the electrical grid. This work aims to detecting the faults occurring in the PV array and, with reference to Table 1, eleven different fault are investigated.

It is worthy to mention that PS conditions used in this work corresponds to an irradiance level affects all examined PV modules. Thus, during the experiments, all examined PV modules were tested under the same PS conditions with different shading percentages (20%, 30%, etc.).

TABLE 1
DIFFERENT TYPE OF FAULTS OCCURRING IN THE EXAMINED PV PLANT

Type of Fault	Symbol
Normal Operation and PS effects the PV system	F1
One faulty PV module	F2
Two faulty PV modules	F3
Three faulty PV modules	F4
Four faulty PV modules	F5
One faulty PV module and PS effects the PV system	F6
Two faulty PV modules and PS effects the PV system	F7
Three faulty PV modules and PS effects the PV system	F8
Four faulty PV modules and PS effects the PV system	F9
Faulty PV String	F10
Faulty MPPT unit	F11

3. *METHODOLOGY*

This section reports the PV data acquisition system, PV theoretical modelling, the overall fault detection algorithm, and the detailed design of the proposed artificial neural network and the fuzzy logic interface system.

3.1 *PV Plant and data Acquisition*

The PV system used in this work consists of a grid-connected PV plant comprising 5 polycrystalline silicon PV modules each with a nominal power of 220 Wp. The photovoltaic modules are connected in series. The photovoltaic string is connected to a Maximum Power Point Tracker (MPPT) with an output efficiency of not less than 95.0% [31 & 32]. The DC current and voltage are measured using the internal sensors which are part of the Flexmax MPPT unit.

A Vantage Pro monitoring unit is used to receive the Global solar irradiance measured by the Davis weather station which includes a pyranometer. A Hub 4 communication manager is used to facilitate acquisition of modules' temperature using the Davis external temperature sensor, and the electrical data for each photovoltaic string. VI LabVIEW software is used to implement data logging and monitoring functions of the PV system. Fig. 2 illustrates the overall system architecture of the PV plant.

The real-time measurements are taken by averaging 60 samples, gathered at a rate of 1 Hz over a period of one minute. Therefore, the obtained results for power, voltage and current are calculated at one minute intervals.

The SMT6 (60) P solar module manufactured by Romag, has been used in this work. The electrical characteristics of the solar module are shown in Table 2. The standard test condition (STC) for these solar panels are: solar irradiance = 1000 W/m^2, module temperature = 25 °C

TABLE 2
ELECTRICAL CHARACTERISTICS OF SMT6 (60) P PV MODULE

Solar Panel Electrical Characteristics	Value
Peak Power	220 W
Voltage at maximum power point (V_{mp})	28.7 V
Current at maximum power point (I_{mp})	7.67 A
Open Circuit Voltage (V_{OC})	36.74 V
Short Circuit Current (I_{sc})	8.24 A
Number of cells connected in series	60
Number of cells connected in parallel	1
Rs , Rsh	0.53 Ohms , 1890 Ohms
dark saturation current (Io)	2.8×10^{-10} A
Ideal diode factor (A)	1.5
Boltzmann's constant (K)	1.3806×10^{-23} J.K^{-1}

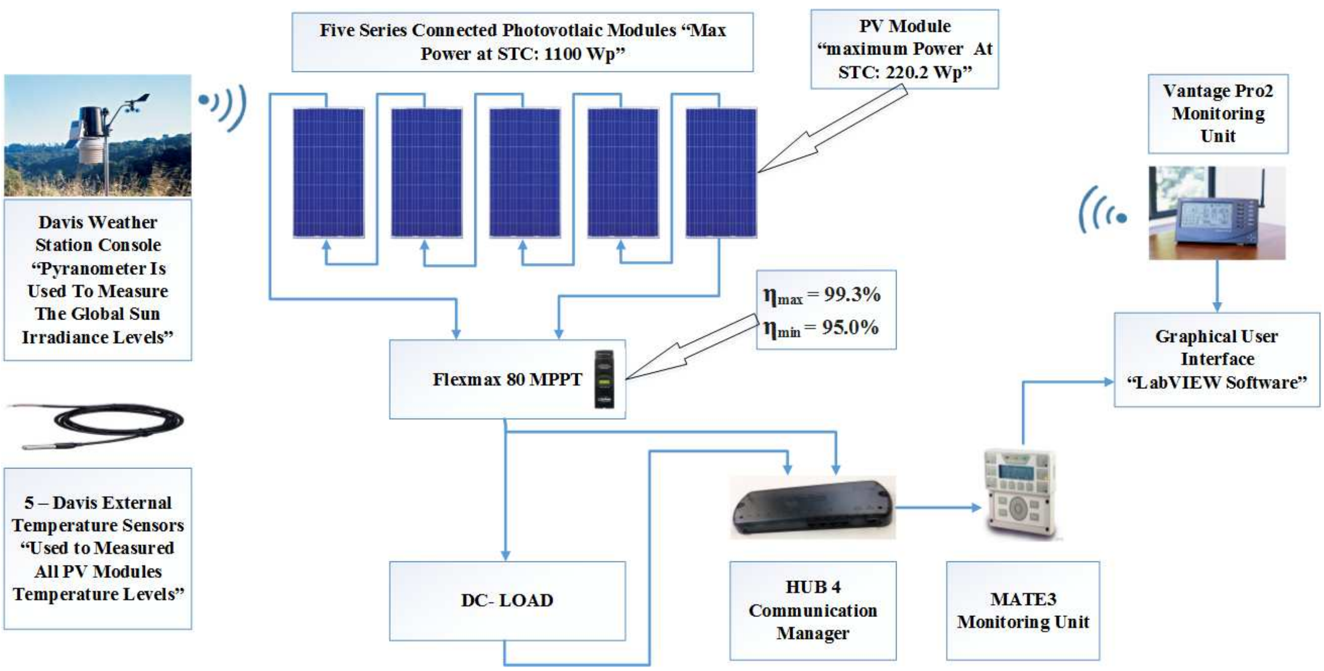

Fig. 2. Examined PV System Installed at the Huddersfield University, United Kingdom

3.2. *Photovoltaic Theoretical Modelling*

The DC side of the PV system is modelled using the 5-parameter model. The voltage and current characteristics of the PV module can be obtained using the single diode model [29] as follows:

$$I = I_{ph} - I_o\left(e^{\frac{V+IR_S}{N_S V_t}} - 1\right) - \left(\frac{V+IR_S}{R_{sh}}\right) \quad (1)$$

where I_{ph} is the photo-generated current at STC , I_0 is the dark saturation current at STC, R_s is the module series resistance, R_{sh} is the panel parallel resistance, N_s is the number of series cells in the PV module and V_t is the thermal voltage and it can be defined based on:

$$V_t = \frac{A\,K\,T}{q} \tag{2}$$

where A the ideal diode factor, k is Boltzmann's constant and q is the charge of the electron.

The five parameter model is determined by solving the transcendental equation (1) using Newton-Raphson algorithm [30] based only on the datasheet of the available parameters for the examined PV module that was used in this work as shown in Table 1. The power produced by the PV module in watts can be easily calculated along with the current (I) and voltage (V) that is generated by equation (1), therefore:

$$P_{theoretical} = I \times V \tag{3}$$

The Current-Voltage (I-V) and Power-Voltage (P-V) curves of the examined PV module is shown in Fig. 3(A) and Fig. 3(B) respectively. Three different simulation results is explained at 1000, 500, and 100 W/m^2. However, the simulation temperature remains at STC (25 °C).

The purpose of using the analysis for the I-V and P-V curves, is to generate the expected output power of the examined PV module, therefore, it can be used to predict the error between the real-time long-term PV measured data and the theoretical power and voltage performance.

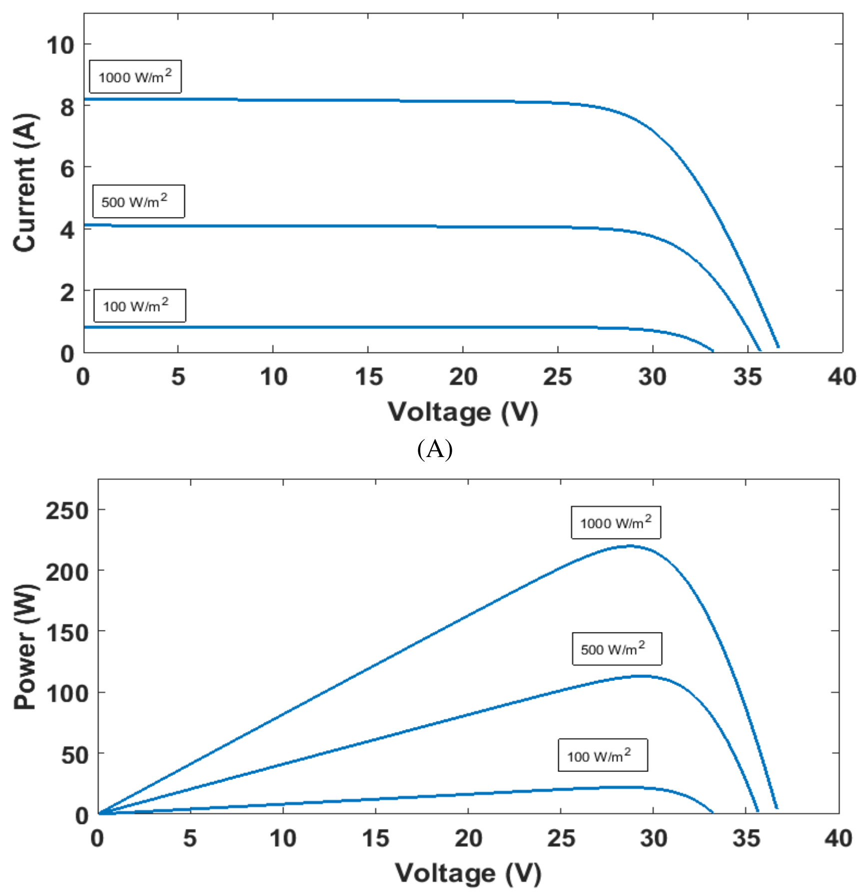

Fig. 3. Photovoltaic Theoretical Curves Modelling. (A) I-V Curve. (B) P-V Curve

3.3 *Overall PV Fault Detection Algorithm*

In order to determine the type of a fault occurred in our PV plant, two ratios have been identified. Power ratio (PR) and voltage ratio (VR) have been used to categorise the region of the fault because both ratios have the following features:

1) Both ratios are changeable during faulty conditions in the PV system
2) When the power ratio is equal to zero, the voltage ratio can still have a value regarding the voltage open circuit of the PV modules

The power and voltage ratios are given by the following expressions:

$$\mathrm{PR} = \frac{\mathrm{P_{theoretical}}}{\mathrm{P_{measured}}} \tag{4}$$

$$\mathrm{VR} = \frac{\mathrm{V_{theoretical}}}{\mathrm{V_{measured}}} \tag{5}$$

where $P_{theoretical}$ is the theoretical output power generated by the PV system, $P_{measured}$ is the measured output power from PV string, $V_{theoretical}$ is the theoretical output voltage generated by the PV system and $V_{measured}$ is the measured output DC voltage from PV string.

Since the internal sensors of the MPPT have a conversion error rate of 95% as shown in Fig. 2, the power ratios are calculated at 5% error tolerance of the theoretical power which presents the maximum error condition for the examined PV system. Therefore, the maximum and minimum power and voltage ratios are expressed by the following formulas which contains the tolerance rate of the MPPT units and the total number of PV modules in the PV string:

$$\mathrm{PR\ min} = \frac{\mathrm{P_{theoretical}}}{\mathrm{P_{measured}}} \tag{6}$$

$$\mathrm{PR\ max} = \frac{\mathrm{P_{theoretical}}}{\mathrm{P_{measured}} \times \mathrm{MPPT\ Tolerance\ Rate}} \tag{7}$$

$$\mathrm{VR\ min} = \frac{\mathrm{V_{theoretical}}}{\mathrm{V_{measured}}} \tag{8}$$

$$\mathrm{VR\ max} = \frac{\mathrm{V_{theoretical}}}{\mathrm{V_{measured}} \times \mathrm{MPPT\ Tolerance\ Rate}} \tag{9}$$

The normal operation mode region of the examined PV plant at STC is shown in Fig. 4 case1, the values of the PR can be calculated using (6 & 7) as the following:

$$\mathrm{Normal\ Operation\ Mode} - \mathrm{PR\ min} = \frac{\mathrm{P_{theoretical}}}{\mathrm{P_{measured}}} = \frac{1100}{1100} = 1$$

$$\mathrm{Normal\ Operation\ Mode} - \mathrm{PR\ max} = \frac{\mathrm{P_{theoretical}}}{\mathrm{P_{measured}} \times \mathrm{MPPT\ Tolerance\ Rate}} = \frac{1100}{1100 \times 95\%} = 1.053$$

As can be noticed from Fig. 4 case 2, the maximum partial shading condition detected by the irradiance sensor is equal to 97.3%, therefore, the maximum PR is calculated as the following:

$$\mathrm{Fault\ Detection\ Algorithm\ Maximum\ PR} = \frac{\mathrm{P_{theoretical}}}{\mathrm{P_{measured}} \times \mathrm{MPPT\ Tolerance\ Rate}} = \frac{1100}{23.66 \times 95\%} \approx 50$$

The value of the maximum PR is important because if the PR is greater than 50, then the fault detection algorithm can specify whether a fault occurred in the MPPT unit or there is a complete disconnection of a PV string from the entire PV system. In order to detect which type of fault accrued in the region of PR > 50. The value of the voltage ratio has been considered, two conditions is selected:

1. If VR $\geq$ 0, then a faulty PV string is detected
2. If VR = 0, then a faulty MPPT unit is detected

Furthermore, if the value of the PR does not lie within the normal operation mode region and it is not higher than the PR max threshold (PR $\geq$ 50), then the value of the PR and VR is passed to the second part of the fault detection algorithm which consists of two different machine learning techniques as shown in Fig. 5.

The first technique is the artificial neural network (ANN). In order to select the most suitable ANN model structure, four different ANN models have been developed:

- 2 Inputs, 5 outputs using 1 hidden layers
- 2 Inputs, 5 outputs using 2 hidden layers
- 2 Inputs, 9 outputs using 1 hidden layers
- 2 Inputs, 9 outputs using 2 hidden layers

A brief illustration on the selection of the variables and ANN model structure is covered in the next section (section 3.4).

The second machine learning technique used to detect possible faults occurring in the PV system is the fuzzy logic. In this paper, two different fuzzy logic systems have been implemented:

- Mamdani-type fuzzy logic system interface
- Sugeno-type fuzzy logic system interface

The fuzzy logic systems are explained in section 3.5. Moreover, the type of the fault which can be detected using the machine learning techniques are shown in Table 1.

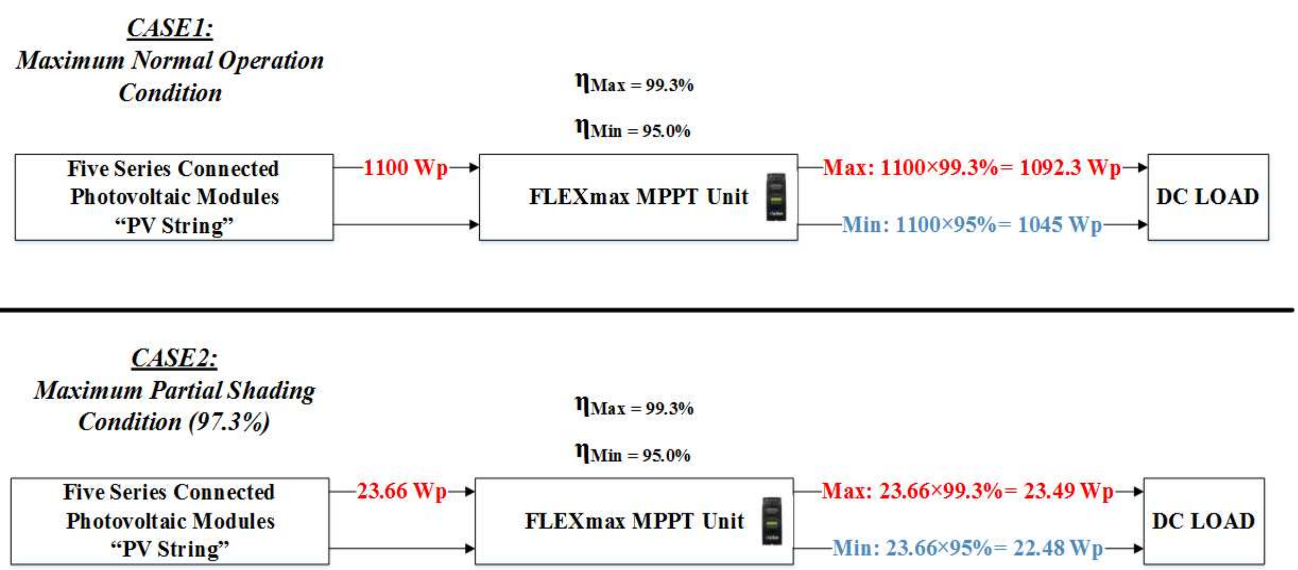

Fig. 4. DC side Numerical Calculations at Maximum and Minimum Operating Points

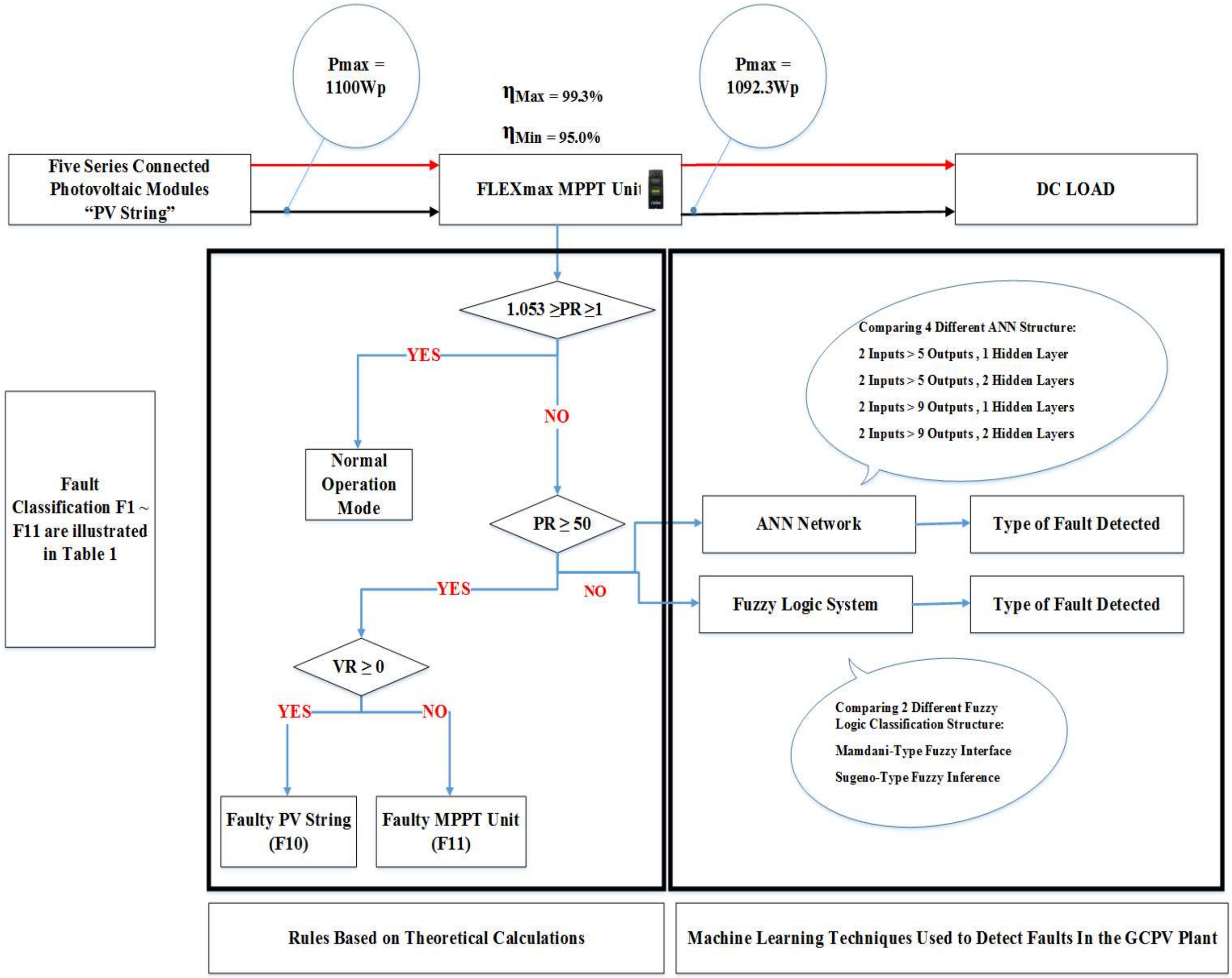

Fig. 5. Detailed PV Fault Detection Approach

3.4 ANN Model Implementation

The main objective of the ANN model is to detect possible faults in the examined PV system shown in Fig. 2. The ANN model has been developed as follows:

- Selection of input and output variables
- Data set normalization
- Selection of network structure
- Network training
- Network test

The input parameters used to configure all tested ANN models are the VR and PR ratios which can be calculated using (8 & 9) respectively. The Data set (input variables) are normalized within the range of -1 and +1 using (10).

$$y = \frac{(y_{max} - y_{min})(x - x_{min})}{(x_{max} - x_{min})} + y_{min} \quad (10)$$

where $\in \{x_{min}, x_{max}\}$, $y \in \{y_{min}, y_{max}\}$ and x is the original data value and y is the corresponding normalized value with $y_{min} = -1$ and $y_{max} = +1$.

In order to select the most efficient architecture for the ANN model, a comparison between four different ANN models have been performed where the structure of all tested ANN networks is the Radial Basis Function (RBF) as shown in Fig. 6.

ANN models A and B are using 2 inputs (VR & PR) and five outputs, where the hidden layers are equal to one and two respectively. The purpose of increasing the hidden layers, is to increase the computational performance of the ANN network, thus, increasing the detection accuracy (DA) of the ANN model. The faults which can be detected using both ANN models are:

- F1: Partial Shading (PS) affecting the PV system
- F2: One faulty PV Module and PS affecting the PV system
- F3: Two faulty PV Modules and PS affecting the PV system
- F4: Three faulty PV Modules and PS affecting the PV system
- F5: Four faulty PV Modules and PS affecting the PV system

From the research conducted using several days measurements (briefly described in the results section), the comparison between model A and model B shows that both models have a low detection accuracy where the maximum achieved detection accuracy is equal to 77.7%. Therefore, this challenge was solved by adding new types of faults for the ANN network that allows the ANN model to detect faulty PV modules only (No PS on the entire PV plant).

ANN models C and D are using 2 inputs (VR & PR) and nine outputs, where the hidden layers are equal to one and two respectively. The faults which can be detected using both ANN models are:

- F1: PS affecting the PV system
- F2: One faulty PV Module only
- F3: Two faulty PV Modules only
- F4: Three faulty PV Modules only
- F5: Four faulty PV modules only
- F6: One faulty PV Module and PS affecting the PV system
- F7: Two faulty PV Modules and PS affecting the PV system
- F8: Three faulty PV Modules and PS affecting the PV system
- F9: Four faulty PV Modules and PS affecting the PV system

In this study, the data set have been recorded from the experimental setup shown in Fig. 2. The data set used to train, validate, and test the ANN networks contains 6480 measurements logged in 9 days as shown in Fig. 7, where each day consists of 720 sample. During the experiment, the PV modules' temperature is between 15.3 – 16.7 ^{o}C, the value of the VR and PR have been logged. Each day has a different fault applied to the PV systems which can be simplified by the following:

- Day 1: Partial shading conditions affecting the PV system
- Day 2: One PV module has been disconnected from the PV system (faulty PV modules)
- Day 3: Two PV modules have been disconnected from the PV system
- Day 4: Three PV modules have been disconnected from the PV system
- Day 5: Four PV modules have been disconnected from the PV system
- Day 6: One PV module has been disconnected and PS applied to all other PV modules
- Day 7: Two PV modules have been disconnected and PS applied to all other PV modules
- Day 8: Three PV modules have been disconnected and PS applied to all other PV modules
- Day 9: Four PV modules have been disconnected and PS applied to all only existing PV module

The obtained measurements is then divided into three subsets:

1. 70% of the data are used to train the ANN networks.
2. 10% of samples are used to validate the ANN network. This test is not used in the training process.
3. 20% of samples are used to test the actual ANN network detection accuracy.

The implementation of the ANN network has been developed using MATLAB/Simulink software. ALL results obtained from the ANN network is discussed briefly in the results section, where the maximum obtained detection accuracy among all tested ANN models is equal to 92.1% for the ANN model which contains 2 inputs, 9 outputs using 2 hidden layers. Moreover, the minimum Mean Square Errors (MSE) achieved during the training and test processes are 0.005 and 0.007 respectively.

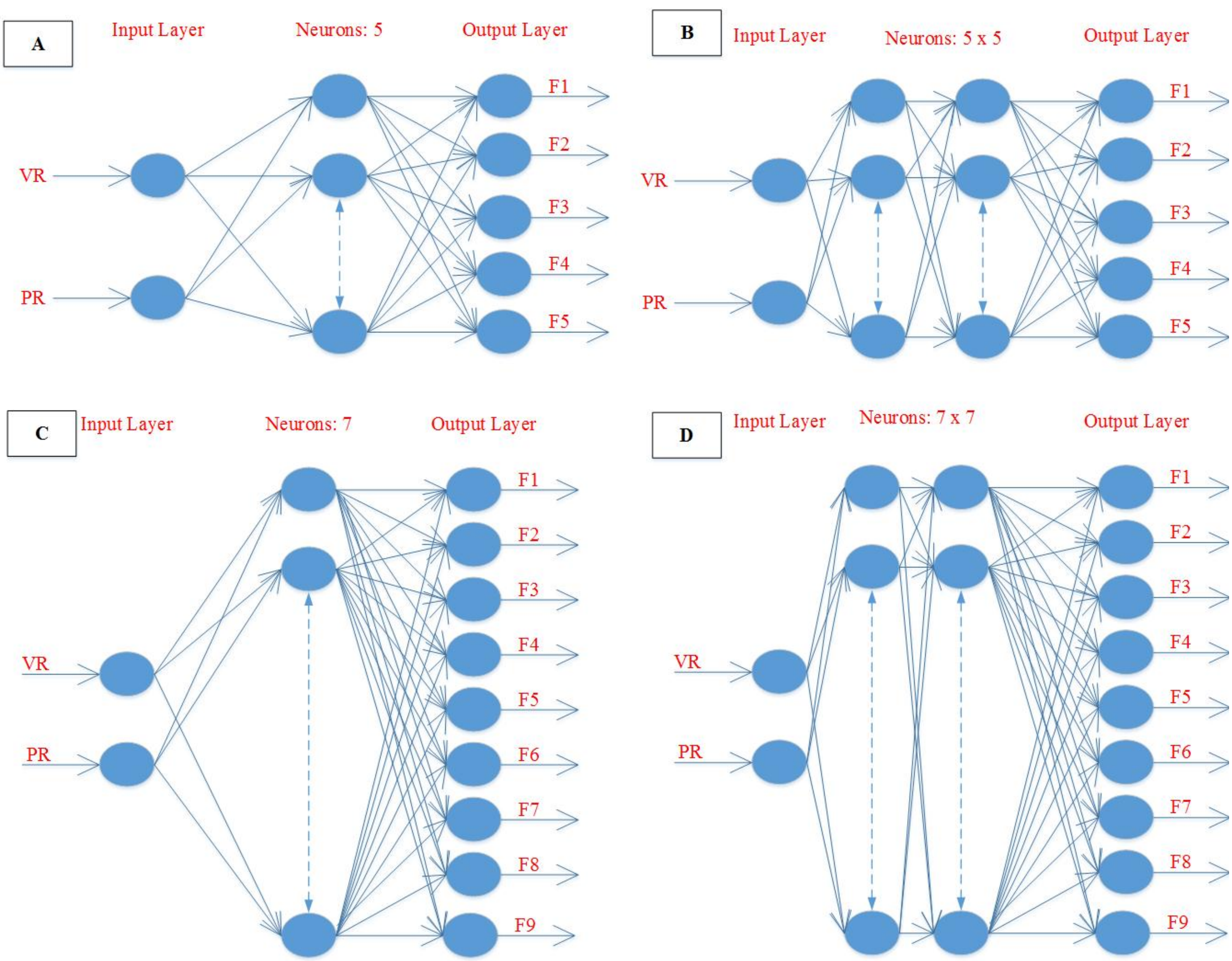

Fig. 6. The Adopted ANN Network. (A) 2 Inputs, 5 Outputs using 1 Hidden Layer, (B) 2 Inputs, 5 Outputs using 2 Hidden Layers, (C) 2 Inputs, 9 Outputs using 1 Hidden Layer, (D) 2 Inputs, 9 Outputs using 2 Hidden Layers

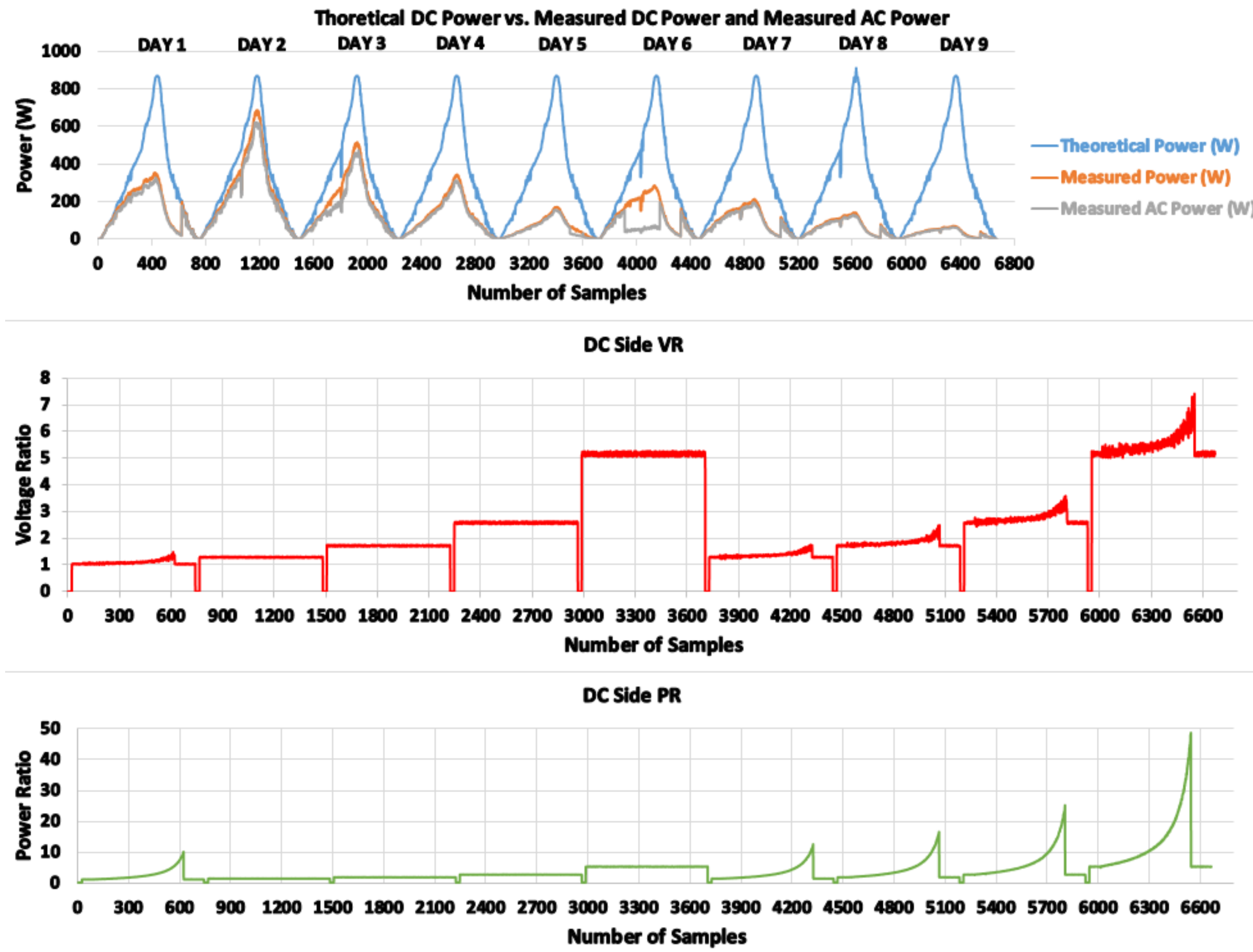

Fig. 7. Dataset used to Train and Validate the ANN networks

3.5 Fuzzy Logic Model Implementation

In this study, the second machine learning technique used to detect faults in the PV system is the fuzzy logic system interface. In order to select the most efficient model for the fuzzy logic system fault detection interface, a comparison between two fuzzy models widely utilized for the classification of faults have been performed: Mamdani fuzzy logic and Sugeno type fuzzy system.

Mamdani fuzzy logic systems commonly suited to human input interface. However, the Sugeno fuzzy systems are well established using a linear weighted mathematical expressions. The main advantages for both fuzzy logic systems are illustrated by the following:

<u>Sugeno-type:</u>

- It is computational efficient.
- It works well with linear techniques.
- It works well with optimization methods and Adaptive techniques.
- It has guaranteed continuity of the output Interface surface.

<u>Mamdani-type:</u>

- It is intuitive.
- It has widespread acceptance.
- It is well suited to human input systems interface

Both implemented fuzzy logic systems are shown in Fig. 8. The VR and PR ratios are used as input variables for the fuzzy logic classification system, where VR and PR is calculated using (7 & 9) respectively. The VR and PR regions are illustrated in Table 3. As can be noticed, ten different regions have been selected, where region 1 is the low partial shading (PS) condition. Whereas, region 4 is used for a faulty PV module with high PS condition (50% ~ 97.3% PS). The minimum and maximum limits for each region of the VR and PR is also shown in Table 3, the defuzzification process for the input rules is the centroid type.

All measurements for the theoretical VR and PR have been taken from a MATLAB/Simulink model which is designed the same as the examined PV system presented in Fig. 2 with the consideration of all PV parameters given in Table 2.

After identifying the input variables VR and PR regions, it is required to set the rulers for the fuzzy logic system interface. As shown in Fig 8, Mamdani fuzzy logic system consists of ten different membership functions (MF) which are described by the following:

- MF1: Low PS affecting the PV system
- MF2: High PS affecting the PV system
- MF3: One faulty PV module and low PS affecting the PV system
- MF4: One faulty PV module and high PS affecting the PV system
- MF5: Two faulty PV modules and low PS affecting the PV system
- MF6: Two faulty PV modules and high PS affecting the PV system
- MF7: Three faulty PV modules and low PS affecting the PV system
- MF8: Three faulty PV modules and high PS affecting the PV system
- MF9: Four faulty PV modules and low PS affecting the PV system
- MF10: Four faulty PV modules and high PS affecting the PV system

The Mamdani based system architecture is using the Max-Min composition technique with a centroid type defuzzification process.

TABLE 3
FUZZY LOGIC INPUT REGIONS – VR & PR

Scenario	Partial Shading %	Min Voltage (V)	Max Voltage (V)	Min Power (W)	Max Power (W)	Fuzzy Classification System Region
Partial Shading (PS)	0 - 49%	1	1.2	1	2.4	1
	50 - 97.3%	1.1	1.4	2.1	28	2
Faulty PV Module and PS	0 - 49%	1.26	1.5	1.3	3	3
	50 - 97.3%	1.34	1.7	2.7	35	4
2 Faulty PV Module and PS	0 - 49%	1.67	1.95	1.8	4	5
	50 - 97.3%	1.76	2.26	3.5	47	6
3 Faulty PV Module and PS	0 - 49%	2.52	2.93	2.5	5.9	7
	50 - 97.3%	2.65	3.4	5.3	70	8
4 Faulty PV Module and PS	0 - 49%	5	5.9	5	12	9
	50 - 97.3%	5.3	6.8	10.6	141	10

Similarly, the fuzzy logic rules obtained for the Sugeno type fuzzy logic interface is equal to 10 as shown in Fig. 8. Where each rule presents the same rule as described in the Mamdani fuzzy logic system. The Sugeno based system architecture is using the Max-Min composition technique with a centroid type defuzzification process.

It is worth pointing out that a high number of fuzzy logic rules ensure both completeness and appropriate resolution of the fault detection accuracy. However, a high number of fuzzy rules may lead to an over parameterized system, thus reducing generalization capability and accuracy of detection the type of the fault accruing in the examined PV system. Therefore, the number of fuzzy rules depends on the number of input variables, system performance, the execution time and the membership functions. In this paper, ten fuzzy logic rules were decided according to a sensitivity analysis made by varying the number and type of the rule. A satisfactory level of performance was obtained after a tuning process, i.e. starting from faulty PV module only and progressively modifying the fuzzy system to detect all possible faults the may occur in the PV plant according to the faults types listed in Table 1.

Both fuzzy logic systems rules are based on: if, and statement. The fuzzy rules are briefly listed in Appendix A. Furthermore, the output surface for Mamdani and Sugeno fuzzy logic systems are plotted and represented by a 3D curves as shown in Fig. 9(A) and Fig. 9(B) respectively. Where the x-axis presents the PR ratio, y-axis presents the VR ratio, and the fault detection output is on the z-axis.

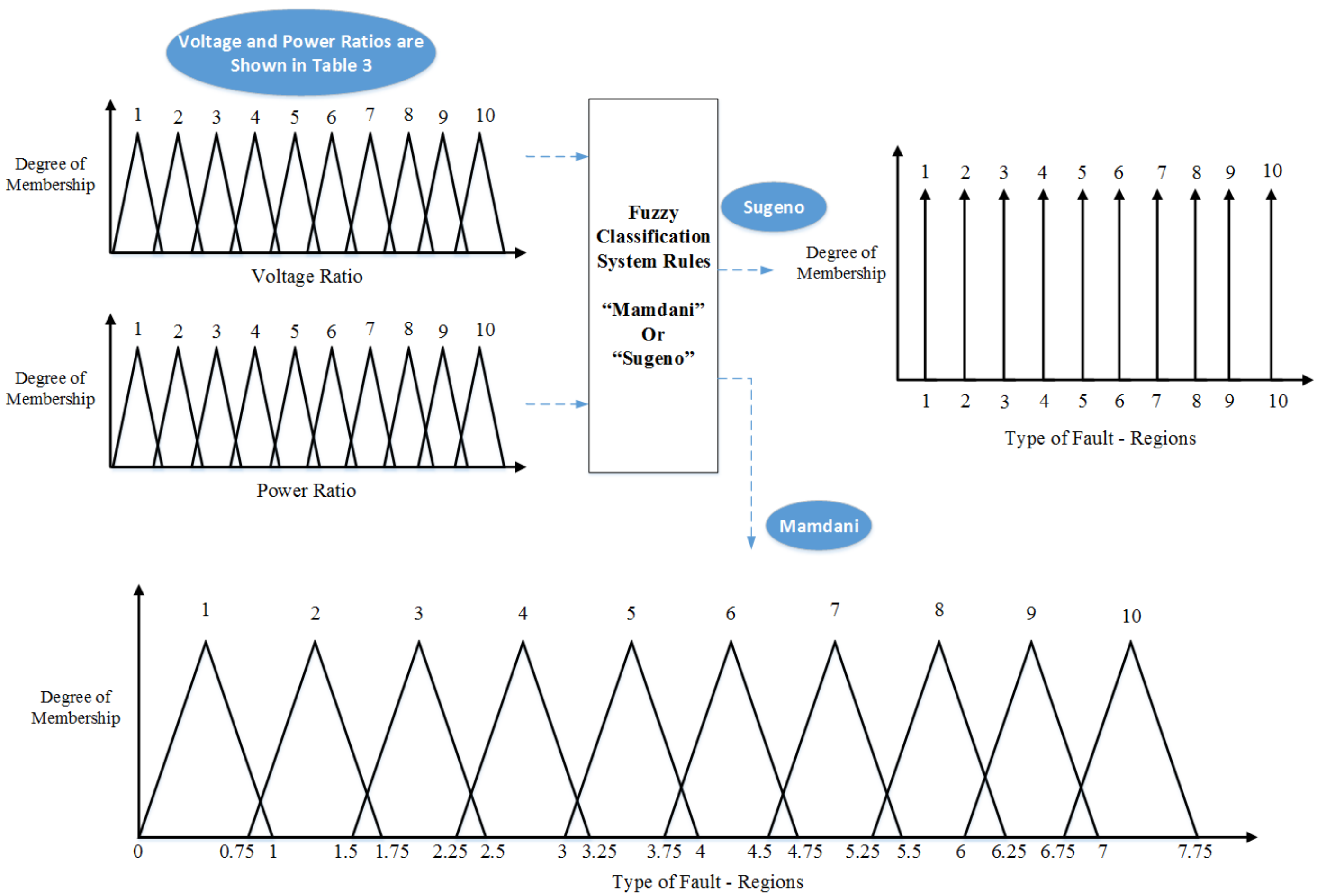

Fig. 8. The Adopted Sugeno and Mamdani Fuzzy Logic Systems

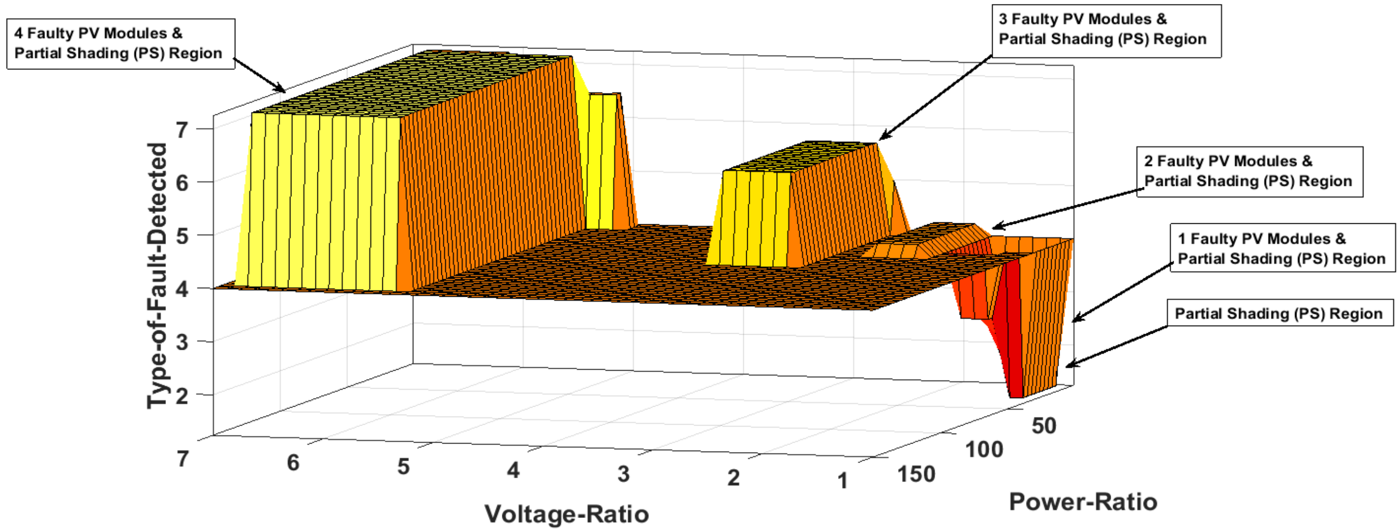

(A)

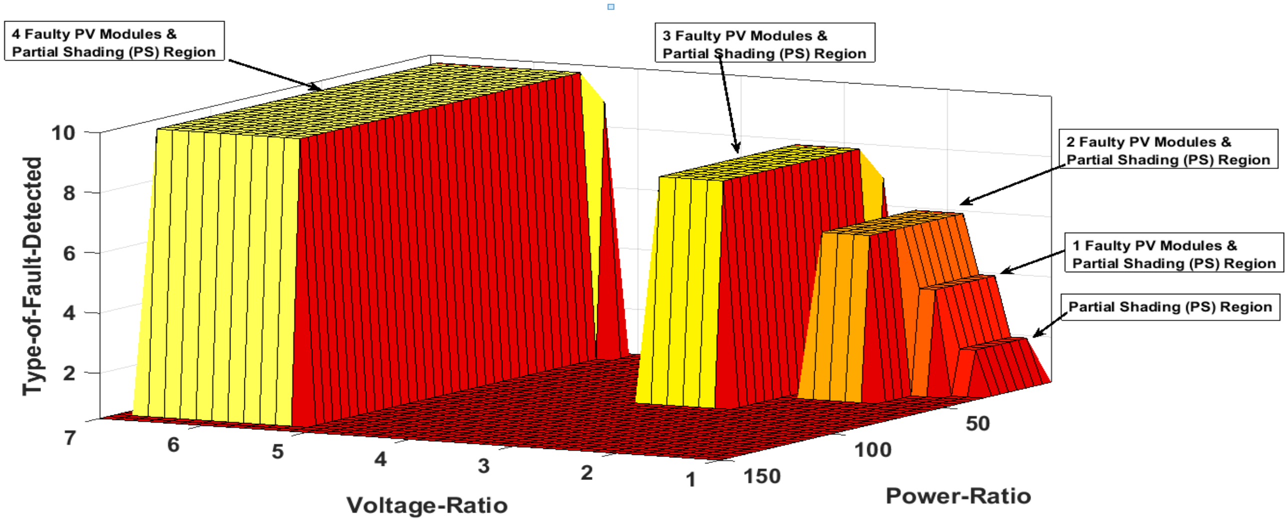

(B)

Fig. 9. Fuzzy Logic Systems Classifier Output Surfaces. (A) Mamdani-Type Fuzzy Logic System Interface, (B) Sugeno-Type Fuzzy Logic System Interface

4. RESULTS AND DISCUSSION

This section reports the results of the developed fault detection algorithm. Furthermore, a comparison between the developed machine learning techniques with some ANN and fuzzy logic systems obtained by various researchers is briefly explained in section 4.4 (discussion section).

4.1 Experimental Data

In order to test the effectiveness of the proposed fault detection algorithm, a number experiments were conducted. Table 4 shows a full day experimental scenarios which are applied to the PV plant, where the perturbation process made to the PV system is shown in Appendix B. Each scenario lasts for an hour and it contains a different condition applied to the examined PV system illustrated previously in Fig. 2.

As can be noticed, the data samples for both sleep and normal operation modes are not included in the evaluation process of the machine learning techniques, since both scenarios can be detecte3d using the mathematical regions explained in Fig. 5. Furthermore, scenarios 3~5 and 7~11 are evaluated by the ANN network and the fuzzy logic system, were the total number of sample for the faulty conditions is equal to four hundred and eighty. Moreover, a comparison between the theoretical output power vs. the real time long term measured data of the PV system during the tested faulty conditions are is shown in Fig. 10.

TABLE 4
MULTIPLE FAULTS OCCURRING IN THE EXAMINED PV SYSTEM

Scenario #	Start time	End time	Condition applied to the PV system	Number of samples applied to the ANN network
1	5:45	5:57	Sleep mode	-
2	5:58	6:59	Normal operation mode	-
3	7:00	7:59	20% partial shading	60
4	8:00	8:59	Faulty PV module and 20% partial shading	60
5	9:00	9:59	Faulty PV module and 40% partial shading	60
6	10:00	10:59	Normal operation mode	-
7	11:00	11:59	2 Faulty PV modules and 30% partial shading	60
8	12:00	12:59	30% partial shading	60
9	13:00	13:59	4 Faulty PV modules only	60
10	14:00	14:59	3 Faulty PV modules and 20% partial shading	60
11	15:00	15:59	3 Faulty PV modules only	60
12	16:00	17:57	Normal operation mode	-
13	17:58	19:00	Sleep mode	-
				Sum: 480

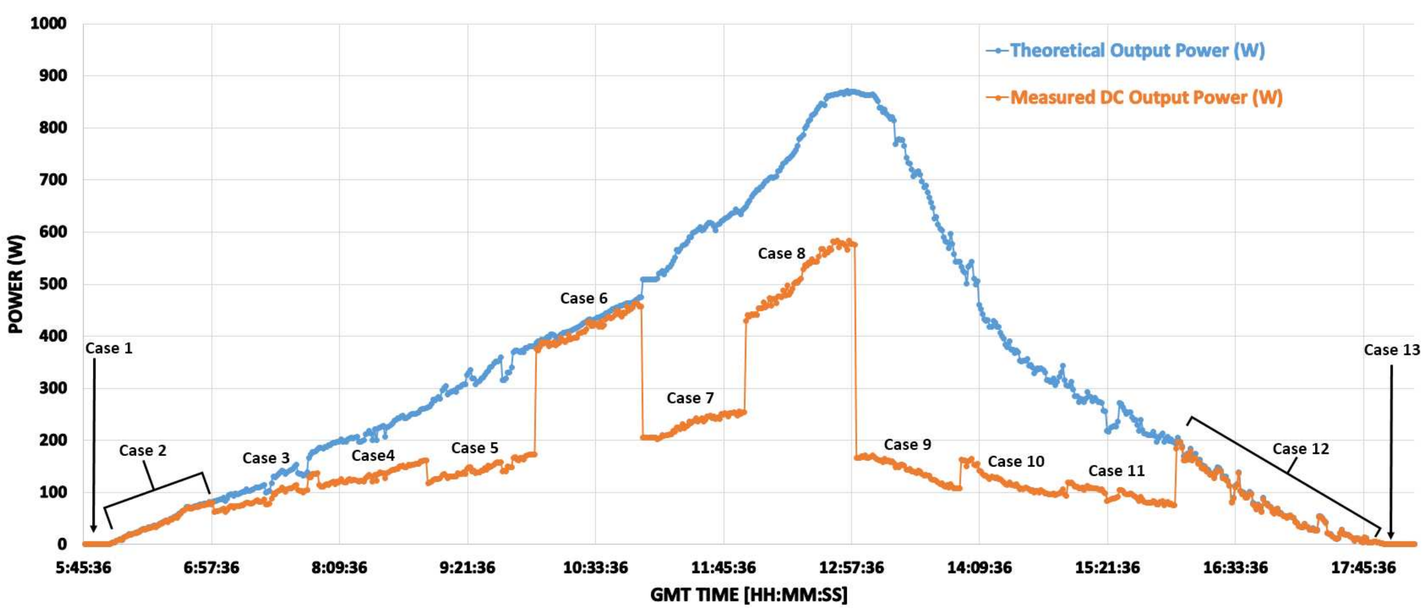

Fig. 10. Theoretical Output Power vs. Measured Output Power for All Tested Scenarios Applied on the Examined PV system, Each Case is Perturbed as Shown in Appendix B

4.2 Performance Evaluation of the proposed ANN Networks

In order to verify the performance of the proposed ANN networks, the VR and PR ratios of 480 samples illustrated in Table 4 have been used as an input for each ANN network shown previously in Fig. 6. For analyzing the effectiveness of each ANN network, Fig 11(A-D) shows the output classification confusion matrices for the developed ANN networks.

The cells of each matrix with red and green colors presents the percentage of faults correctly and not correctly classified by the ANN network respectively. Additionally, the fault classification number, fault type and number of samples for each examined ANN network is shown in Table 5. Moreover, the gray blocks represents the total percentage of the detection accuracy in the column and row respectively.

In order to understand how to read the confusion matrices shown in Fig. 11. The first confusion matrix (Fig. 11(A)) will be explained in brief. In this figure, the first five diagonal cells show the number and percentage of correct classifications by the trained network. For example, 118 samples for F1 (fault type, shown in Table 5), are correctly classified. This corresponds to 24.6% of all tested samples (480 sample). Similarly, 30 samples are correctly classified as F2, this corresponds to 6.3% of all 480 samples.

In row 1, 1 sample is incorrectly classified as F1 and it is classified as F3, this corresponds to 0.2% of all 480 samples. Similarly, 2 samples of F5 are incorrectly classified as F1 and this corresponds to 0.4% of all 480 samples.

In row 2, 30 samples are correctly classified as being F2, this corresponds to 6.3% of all 480 samples.

Out of 120 sample corresponds to row 1, 97.5% are correct and 2.5% are wrong. Out of 120 samples corresponds to column 1, 98.3% are correct and 1.7% are classified incorrectly. For row 2, all samples have been classified correctly, 100%. However, for column 2, out of 120 samples, 25% are correct and 75% are incorrect.

The overall detection accuracy of the confusion matrix could be calculated using the diagonal cells as the following:

$$1^{st}\text{ cell }(24.6\%) + 2^{nd}\text{ cell }(6.3\%) + 3^{rd}\text{ cell }(10.2\%) + 4^{th}\text{ cell }(17.3\%) + 5^{th}\text{ cell }(11.9\%) = 70.2\%$$

This 70.2 corresponds to the percentage of correctly classified samples (out of all tested samples, 480 sample). And 29.8% correspond to incorrectly classified samples.

From the obtained results in Fig. 11(A) the minimum detection accuracy is associated with column 2, where 75% of the samples are incorrectly classified. This situation occurred when 3 faulty PV modules and PS affecting the PV module (F3) is classified as F2. And this happens when there is a rapid drop/increase in the irradiance level or PS conditions affecting the examined PV modules.

Similar results obtained with the second ANN network (contains 2 outputs and 2 hidden layers) shown in Fig. 11(B). Where the percentage of the error in identifying F3 is increased to 83.3%, shown in column 2. However, the overall detection accuracy of the second ANN network is increased to 77.7% comparing to 70.2% obtained by the first ANN network. This increase in the detection accuracy is due to the second hidden layer which enables more training and validation computational process for the ANN network before the testing phase.

As can be noticed, ANN networks one and two have low overall detection accuracy. As mentioned earlier in section 3.4, this challenge was solved by adding new type of faults for the ANN network that allows the ANN model to detect faulty PV modules only (No PS on the entire PV plant).

Fig. 11(C) describes the output classification confusion matrix of the third ANN network (contains 9 outputs and 1 hidden layer). The overall detection accuracy of the ANN network is equal to 87.5% where the highest error is associated with F7 (row 7). This fault is related to the samples of F7 which are classified as F8. This situation occurred when two faulty PV modules with high partial shading condition is detected by the ANN network as three faulty PV modules with low PS condition affecting the entire PV system.

The last ANN network contains 2 inputs, 9 outputs and 2 hidden layers. The overall detection accuracy of the network is 92.1% which means that the ANN network detects accurately 442 samples out of 480, this results is shown in Fig. 11(D).

The highest error in identifying the type of the fault is associated with the samples of F6 being classified as F1. The total percentage of error is equal to 10.3%, shown in column 1. Out of 120 samples, 8 sample are incorrectly classified. This situation occurred when there is a high partial shading conditions applied to the PV system including one faulty PV module. Based on the detected samples, this type of the fault is classified as being F1 (PS affecting the PV system).

In conclusion, the obtained results of this section shows that the maximum detection accuracy of all examined ANN networks is equal to 92.1% which is achieved by the fourth ANN network that includes 2 inputs, 9 outputs with 2 hidden layers.

TABLE 5

FAULTS ASSOCIATED WITH THE EXAMINED ANN NETWORKS

ANN network	Fault number	Type of the fault	Number of samples
ANN network 1 and 2 as shown in Fig. 11(A) and Fig. 11(B) respectively	F1	PS affecting the PV system	120
	F2	1 Faulty PV module & PS affecting the PV module	120
	F3	2 Faulty PV modules & PS affecting the PV module	60
	F4	3 Faulty PV modules & PS affecting the PV module	120
	F5	4 Faulty PV modules & PS affecting the PV module	60
ANN network 3 and 4 as shown in Fig. 11(C) and Fig. 11(D) respectively	F1	PS affecting the PV system	120
	F2	1 Faulty PV module	0
	F3	2 Faulty PV modules	0
	F4	3 Faulty PV modules	60
	F5	4 Faulty PV modules	60
	F6	1 Faulty PV module & PS affecting the PV module	120
	F7	2 Faulty PV modules & PS affecting the PV module	60
	F8	3 Faulty PV modules & PS affecting the PV module	60
	F9	4 Faulty PV modules & PS affecting the PV module	0

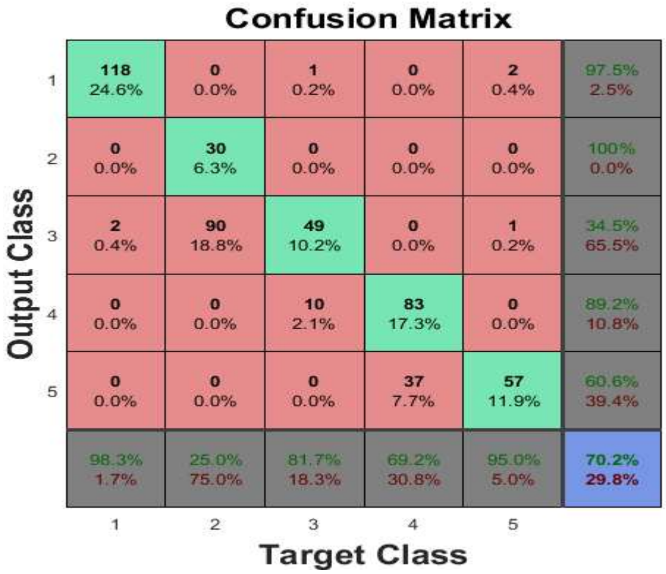

(A)

(B)

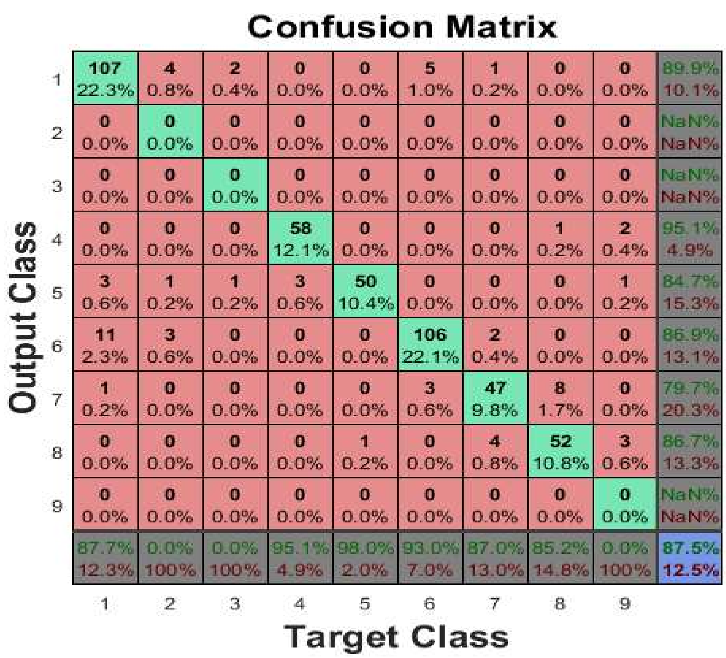

(B)
(C)

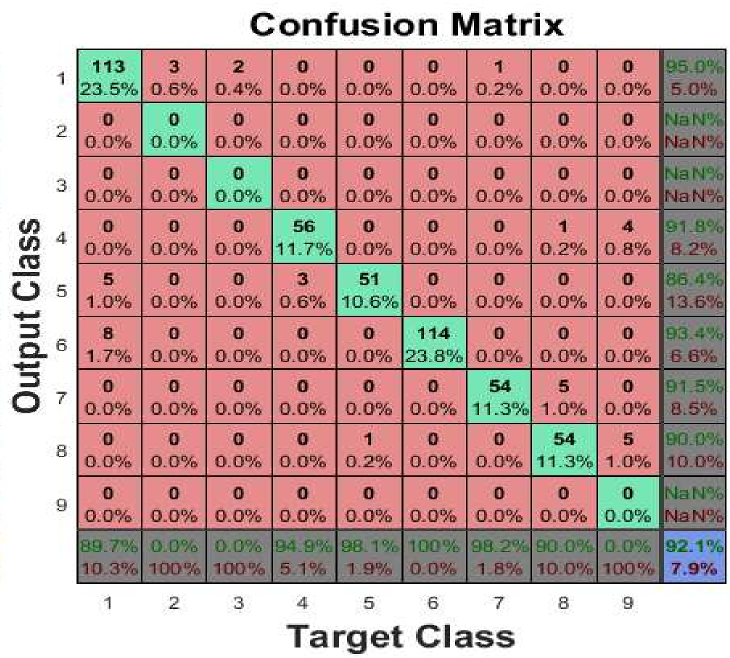

(D)

Fig. 11. Classification Confusion Matrices for the Examined ANN Networks shown previously in Fig. 4. (A) 2 Inputs, 5 Outputs using 1 Hidden Layer, (B) 2 Inputs, 5 Outputs using 2 Hidden Layers, (C) 2 Inputs, 9 Outputs using 1 Hidden Layer, (D) 2 Inputs, 9 Outputs using 2 Hidden Layers

4.3 Performance Evaluation of the proposed Fuzzy Logic Systems

In order to test the effectiveness of the proposed fuzzy logic systems (Mamdani and Sugeno) the faulty samples shown previously in Table 4 have been processed in each fuzzy system. Furthermore, the implementation of the fuzzy logic systems are explained in section 3.5.

A. Mamdani Fuzzy Logic System:

Fig. 12(A) shows the output membership function vs. the faulty samples which are equal to 480 for Mamdani fuzzy logic system interface. Each faulty PV condition is labelled on the figure. As an example, case 3 presents 20% partial shading condition affecting the PV module, for this particular PV faulty scenario, the output of the fuzzy system is equal to 0.5, which is the region of PS condition illustrated in Fig. 12(B). Similarly, case 4 and 5 presents a faulty PV module with 20% and 40% PS respectively. Both cases are within the same membership function region due to the low PS condition affecting the PV modules, this situation is labeled as case 4 and case 5 on both Figs. 12(A) and 12(B).

As can be noticed that all examined faulty conditions are accurately detected by Mamdani fuzzy logic system. However, between case 7 and case 8 there is a small amount of error in detecting the region of the fault, same result accruing between case 8 and case 9. This situation is occurring in the fuzzy system due to the high number of faulty regions identified by the fuzzy system, additionally, the VR and PR ratios are strongly depends on the performance of the voltage and current sensors used to detect the change in the PV parameters (voltage, current and power). Therefore, the fuzzy logic system might need some extra few seconds to start detecting the exact faulty occurring in the PV installation.

B. Sugeno Fuzzy Logic System:

Fig. 13(A) shows the output membership function vs. the faulty samples for Sugeno fuzzy logic system interface. Each faulty PV condition is labelled on the figure. As an example, case 7 presents two faulty PV modules and low partial shading condition affecting the PV plant, for this particular PV faulty scenario, the output of the fuzzy system is equal to 5, which is the region of PS condition illustrated in Fig. 13(B).

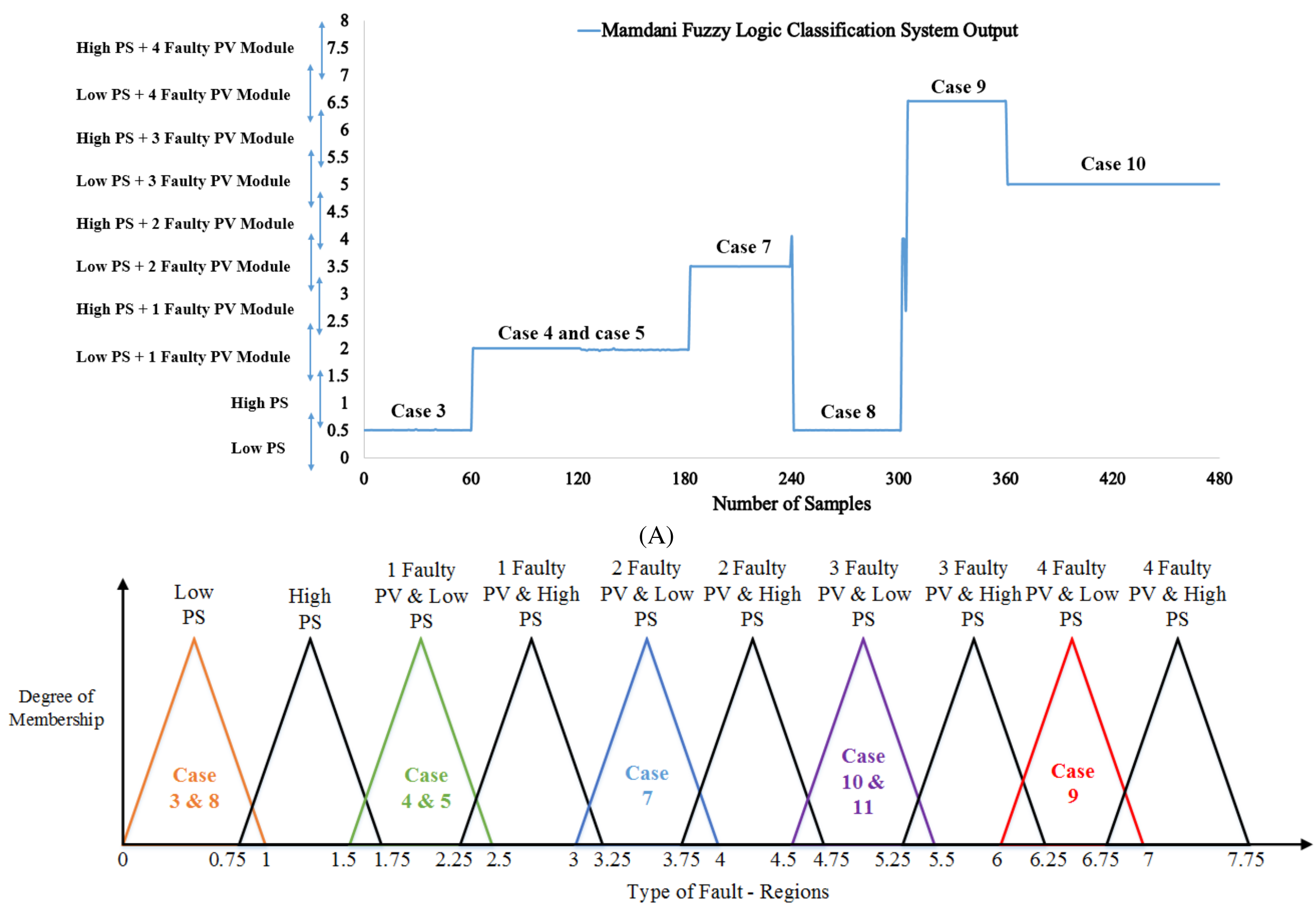

Fig. 12. Output Results Obtained using Mamdani Fuzzy Logic System. (A) Membership Functions vs. Number of Samples, (B) Membership Function Explained Previously in Section 3.5 vs. Type of Fault

Similarly, case 10 and 11 presents a three faulty PV modules with 20% and 0% PS respectively. Both cases are within the same membership function region due to the low PS condition affecting the PV modules, this situation is labeled as case 10 and case 11 on both Figs. 13(A) and 13(B).

From the result obtained by the Sugeno fuzzy logic system, all examined faulty conditions are accurately detected. However, between case 7 and case 8 there is a small amount of error in detecting the region of the fault. This situation is occurring in the fuzzy system due to the high number of faulty regions identified by the fuzzy system, additionally, the VR and PR ratios are strongly depends on the performance of the voltage and current sensors used to detect the change in the PV parameters (voltage, current, and power). Similar error was also observed by the Mamdani fuzzy logic system between case 7 and case 8.

In conclusion, this section presents the behavior of the fuzzy logic systems developed for detecting faulty conditions occurring in the examined PV system. Both fuzzy logic systems show an accurate results in detecting various faults comparing to the results obtained by the ANN networks which has a maximum detection accuracy equals to 92.1%. A comparison between both machine learning techniques are discussed briefly in the following section: 4.4 discussion.

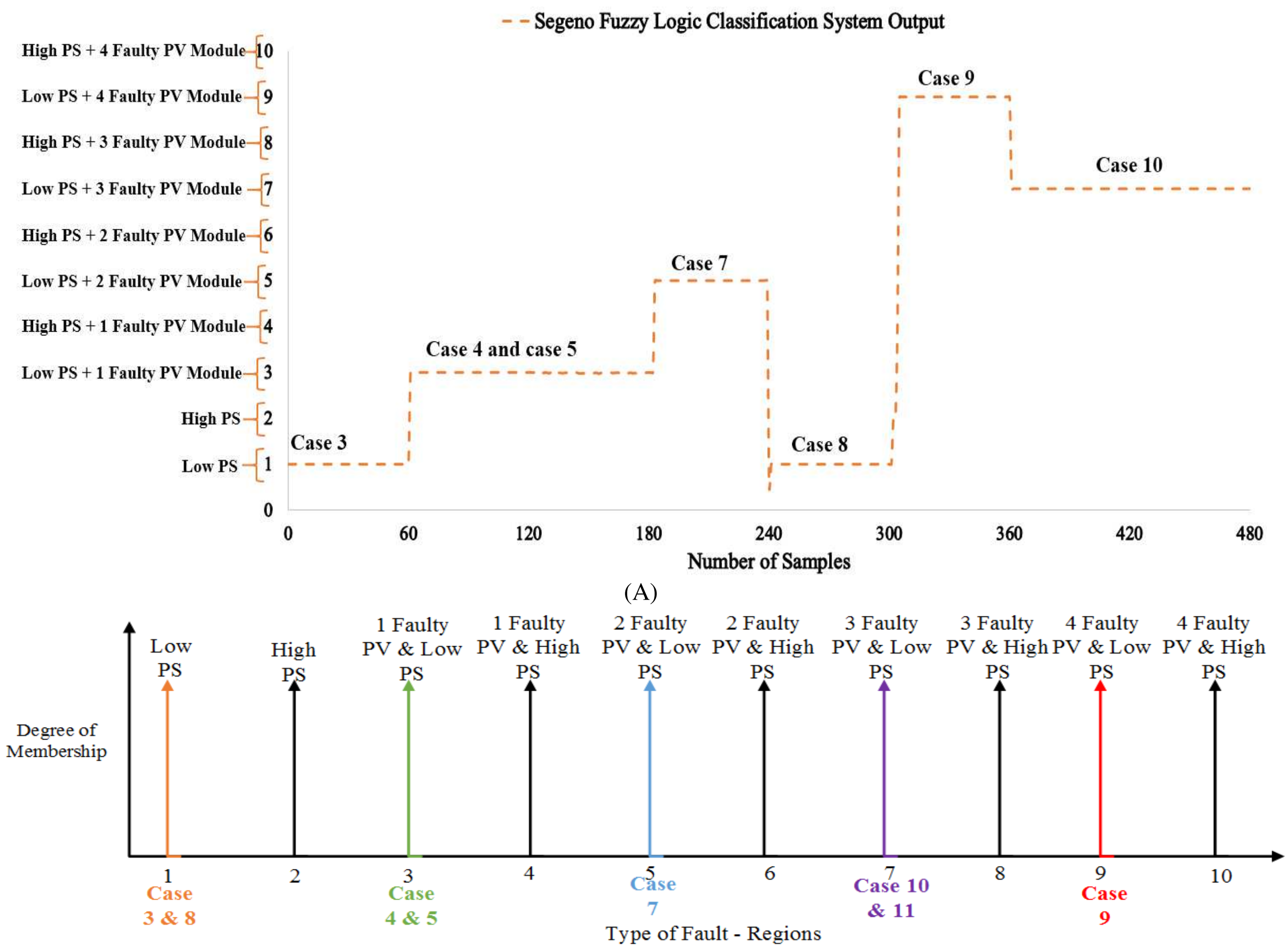

(B)

Fig. 13. Output Results Obtained using Sugeno Fuzzy Logic System. (A) Membership Functions vs. Number of Samples, (B) Membership Function Explained Previously in Section 3.5 vs. Type of Fault

4.4 Discussion

In this study, artificial intelligent network (ANN) and fuzzy logic system interface have been developed for detecting faults in PV installations. However, the PV system used for analyzing the performance of both machine learning techniques is considered as low capacity PV installation (1.1 kWp). For that instance, the output of the fuzzy logic systems shows an accurate detecting accuracy (all examined faults have been detected correctly) comparing to the ANN which has a maximum detection accuracy equals to 92.1% obtained for the fourth ANN structure which contains 2 inputs, 9 outputs using 2 hidden layers. The input membership functions of the fuzzy logic system could be much complicated if the examined PV installation has much more PV modules (~100 PV modules), since each PV module could affect the overall input membership functions.

In order to test the effectiveness of the final detection accuracy obtained by the ANN network. The proposed method has been compared with the ANN output results presented in [25]. The output confusion matrix for both obtained studies are compared in Fig. 14(A) and Fig. 14(B). As can be noticed, the overall detection efficiency of the proposed ANN network is equal to 92.1% comparing to 90.3% obtained by [25]. The faults which are detected by [25] is related to the bypass diodes in the PV systems which is quite different than the faults obtained by this research. However, both ANN networks are using the variations of the voltage and the power form the PV plant as an inputs for the ANN model.

To the best of our knowledge, few of the reviewed articles used a fuzzy logic system to detect faults in PV installations. Therefore, this is one of the novel contribution of this study. A compression between the output membership functions developed by [1] and this study are shown in Fig. 15(A) and Fig. 15(B) respectively. In [1] authors' are using Mamdani fuzzy logic system for enhancing the detection of partial shading conditions effecting the PV plant. The proposed mathematical calculations of the fuzzy logic system is also presented in Fig. 15(A). Moreover, the fuzzy logic systems (Mamdani and Sugeno) presented in this paper are used for detecting possible faults accruing in the examined PV system. The overall detection accuracy of the proposed fuzzy systems is very high, since the examined PV system does not contain too many PV modules.

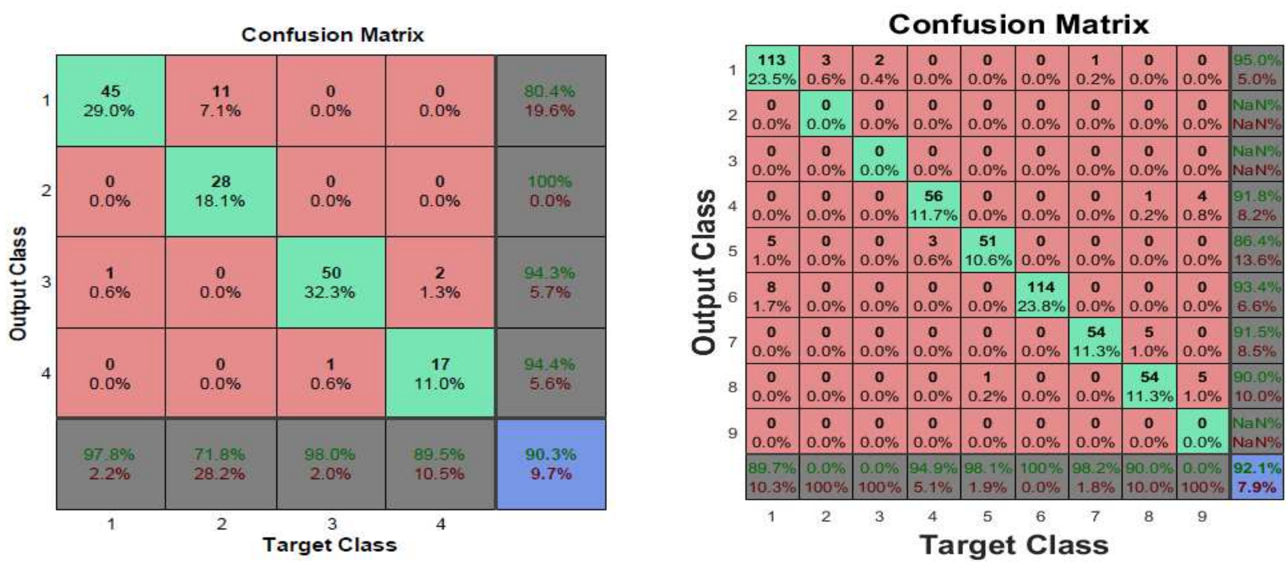

(A) (B)

Fig. 14. Classification Confusion Matrix for ANN Network. (A) Results Obtained by W. Chine et al [25], (B) Results Achieved using the Proposed ANN Fault Detection Algorithm

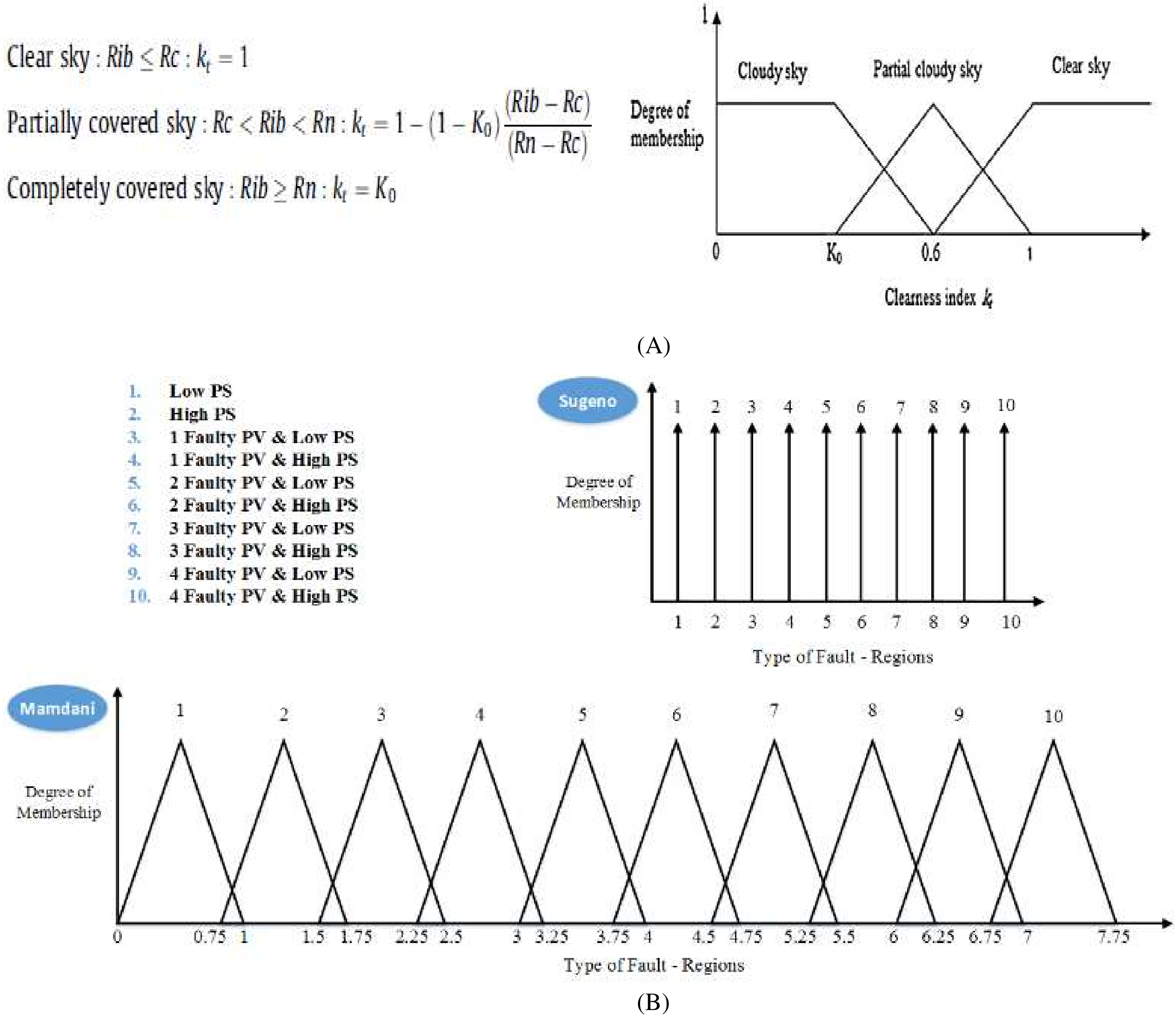

Fig. 15. Fuzzy Logic Models. (A) Membership Functions Proposed by M. Tadj [1], (B) Membership Functions for Mamdani and Sugeno Fuzzy Logic Systems Proposed in this Study

The obtained results for the developed ANN network and the fuzzy logic system are compared in Table 5. The mathematical modelling on the ANN network is much simpler comparing to the creation of the fuzzy logic membership functions, this situation is correct specially for large PV installations. However, the ANN network does require a log of samples in order to validate and train the network while the fuzzy logic systems does not require any log of data before creating the membership function, it just need to update the mathematical modelling with the degradation rates of the MPPT units and/or any other possible source for decreasing the overall efficiency of the PV system such as the DC/AC inverters.

The overall detection accuracy for both machine learning techniques are high if they have been built accurately. Finally, Table 6 shows some of the recent applications for ANN networks and the fuzzy logic systems developed nowadays in PV plants.

TABLE 6

COMPARISON BETWEEN ANN AND FUZZY LOGIC SYSTEMS

Comparison	ANN Network Fault Detection Approach	Fuzzy Logic System Fault Detection Approach
Mathematical Modelling	Does not contain complex mathematical modelling, since it depends on a log of data	For larger PV systems(~100 PV modules) the membership functions does require a lot of mathematical expressions
Detection Accuracy	High	High
Detection Time "Response"	Fast (milli/micro seconds)	Fast (milli/micro seconds)
Photovoltaic Parameters	Depends on the type of the PV fault which needs to be detected	Depends on the type of the PV fault which needs to be detected
Logged Data	Required	Dose not require any previous logged data
Recent Applications Applied to PV Systems	i. Improving the estimation of GCPV power output [33] ii. Forecasting for global solar radiation [34 & 35]	i. Power optimization in standalone PV systems [21] ii. PV fault detection based on multi-resolution signal decomposition [36 & 37]

5. *CONCLUSION*

This paper presents a new photovoltaic (PV) fault detection algorithm which comprises both artificial neural network (ANN) and fuzzy logic system interface. The algorithm is capable for detecting various fault occurring in the PV system such as faulty PV module, two faulty PV modules and partial shading conditions affecting the PV system. Both machine learning techniques was validated using a 1.1 kWp PV plant installed at the University of Huddersfield, United Kingdom.

The fault detection algorithm is using the variations of the voltage and power of the examined PV system as an input for both ANN and the fuzzy logic system. In order to achieve high rate of detection accuracy, four various ANN networks have been tested. The maximum overall detection accuracy was obtained is equal to 92.1% from an ANN network which contains 2 inputs, 9 outputs using 2 hidden layers.

Additionally, two different fuzzy logic systems have been examined. Mamdani fuzzy logic system interface and Sugeno type fuzzy system. Both examined fuzzy logic systems show approximately the same output during the experiments. However, there are slightly difference in developing each type of the fuzzy systems such as the output membership functions and the rules applied for detecting the type of the fault occurring in the PV plant

The developed fault detection algorithm has been discussed and compared with various results obtained from different references in the discussion section. Finally, further investigation of the proposed fault detection algorithm is intended to be used with field programmable gate array (FPGA) platforms which accelerate the speed of detecting possible faults occurring in PV systems.

Appendix A

Fuzzy logic rules applied for both Mamdani and Sugeno fuzzy logic systems interface:

- 1. If (Voltage-Ratio is 1) and (Power-Ratio is 1) then (Type-of-Fault-Detected is 1) (1)
- 2. If (Voltage-Ratio is 2) and (Power-Ratio is 2) then (Type-of-Fault-Detected is 2) (1)
- 3. If (Voltage-Ratio is 3) and (Power-Ratio is 3) then (Type-of-Fault-Detected is 3) (1)
- 4. If (Voltage-Ratio is 4) and (Power-Ratio is 4) then (Type-of-Fault-Detected is 4) (1)
- 5. If (Voltage-Ratio is 5) and (Power-Ratio is 5) then (Type-of-Fault-Detected is 5) (1)
- 6. If (Voltage-Ratio is 6) and (Power-Ratio is 6) then (Type-of-Fault-Detected is 6) (1)
- 7. If (Voltage-Ratio is 7) and (Power-Ratio is 7) then (Type-of-Fault-Detected is 7) (1)
- 8. If (Voltage-Ratio is 8) and (Power-Ratio is 8) then (Type-of-Fault-Detected is 8) (1)
- 9. If (Voltage-Ratio is 9) and (Power-Ratio is 9) then (Type-of-Fault-Detected is 9) (1)
- 10. If (Voltage-Ratio is 10) and (Power-Ratio is 10) then (Type-of-Fault-Detected is 10) (1)

Appendix B

Perturbation process made to test the examined photovoltaic plant:

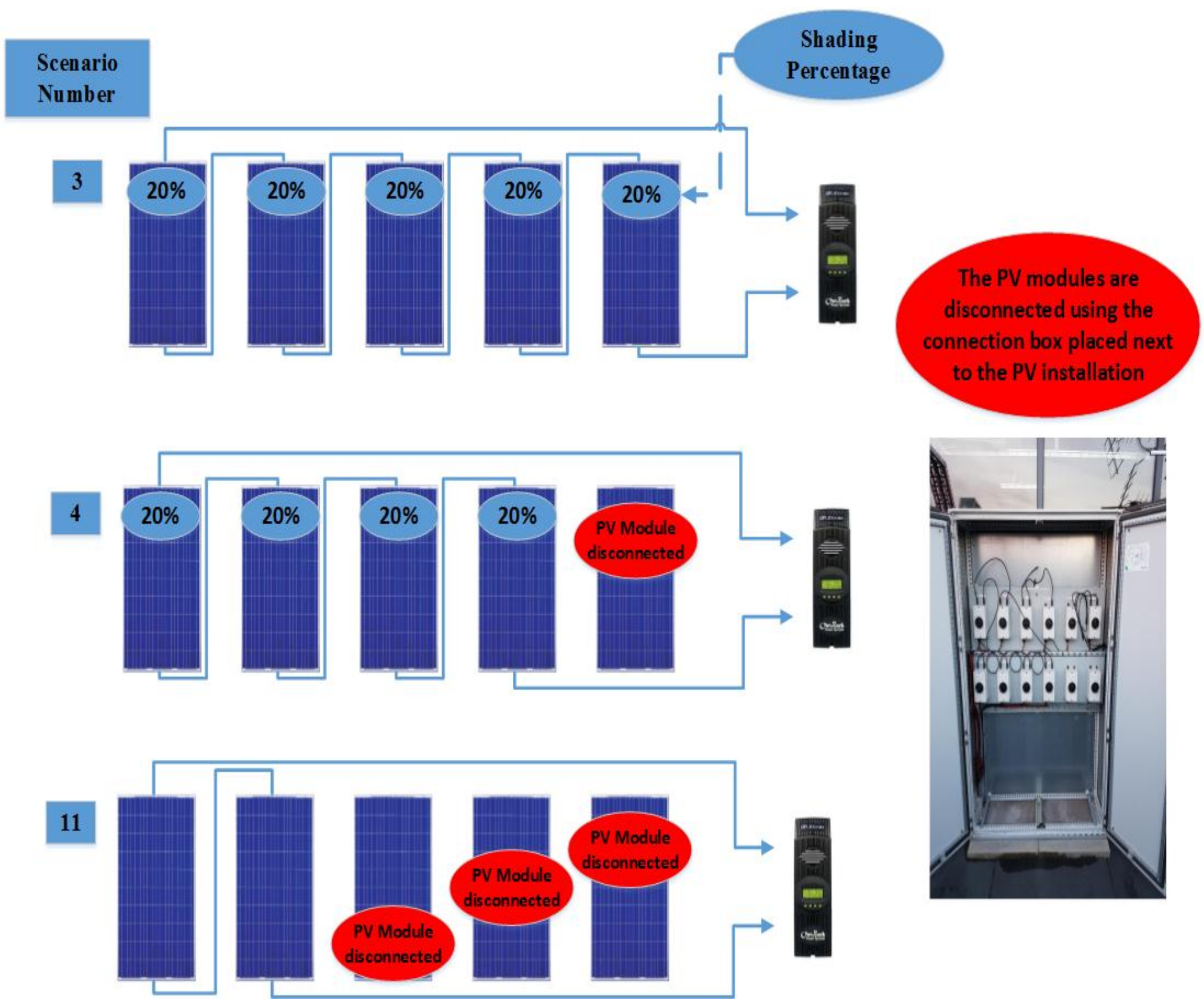

REFRENCES

[1] Tadj, M., Benmouiza, K., Cheknane, A., & Silvestre, S. (2014). Improving the performance of PV systems by faults detection using GISTEL approach. *Energy conversion and management*, *80*, 298-304.

[2] Mellit, A., & Pavan, A. M. (2010). A 24-h forecast of solar irradiance using artificial neural network: Application for performance prediction of a grid-connected PV plant at Trieste, Italy. Solar Energy, 84(5), 807-821.

[3] Takashima, T., Yamaguchi, J., Otani, K., Oozeki, T., Kato, K., & Ishida, M. (2009). Experimental studies of fault location in PV module strings. *Solar Energy Materials and Solar Cells*, *93*(6), 1079-1082.

[4] Dhimish, M., & Holmes, V. (2016). Fault detection algorithm for grid-connected photovoltaic plants. Solar Energy, 137, 236-245.

[5] Silvestre, S., Chouder, A., & Karatepe, E. (2013). Automatic fault detection in grid connected PV systems.

[6] Dhimish, M., Holmes, V., Mehrdadi, B., & Dales, M. (2017). Simultaneous Fault Detection Algorithm for Grid-Connected Photovoltaic Plants. *IET Renewable Power Generation*.

[7] Chine, W., Mellit, A., Pavan, A. M., & Kalogirou, S. A. (2014). Fault detection method for grid-connected photovoltaic plants. Renewable Energy, 66, 99-110.

[8] Silvestre, S., da Silva, M. A., Chouder, A., Guasch, D., & Karatepe, E. (2014). New procedure for fault detection in grid connected PV systems based on the evaluation of current and voltage indicators. Energy Conversion and Management, 86, 241-249.

[9] Dhimish, M., Holmes, V., & Dales, M. (2017). Parallel fault detection algorithm for grid-connected photovoltaic plants. *Renewable Energy*, *113*, 94-111.

[10] Kim, K. A., Seo, G. S., Cho, B. H., & Krein, P. T. (2016). Photovoltaic hot-spot detection for solar panel substrings using ac parameter characterization. IEEE Transactions on Power Electronics, 31(2), 1121-1130.

[11] Obi, M., & Bass, R. (2016). Trends and challenges of grid-connected photovoltaic systems–A review. Renewable and Sustainable Energy Reviews, 58, 1082-1094.

[12] Dhimish, M., Holmes, V., Mehrdadi, B., Dales, M., Chong, B., & Zhang, L. (2017). Seven indicators variations for multiple PV array configurations under partial shading and faulty PV conditions. *Renewable Energy*.

[13] Khamis, A., Shareef, H., Bizkevelci, E., & Khatib, T. (2013). A review of islanding detection techniques for renewable distributed generation systems. Renewable and Sustainable Energy Reviews, 28, 483-493.

[14] Dhimish, M., Holmes, V., Mehrdadi, B., & Dales, M. (2017). The Impact of Cracks on Photovoltaic Power Performance. *Journal of Science: Advanced Materials and Devices*.

[15] Zhao, Y., Yang, L., Lehman, B., de Palma, J. F., Mosesian, J., & Lyons, R. (2012, February). Decision tree-based fault detection and classification in solar photovoltaic arrays. In Applied Power Electronics Conference and Exposition (APEC), 2012 Twenty-Seventh Annual IEEE (pp. 93-99). IEEE.

[16] Jamshidpour, E., Poure, P., & Saadate, S. (2015). Photovoltaic systems reliability improvement by real-time FPGA-based switch failure diagnosis and fault-tolerant DC–DC converter. IEEE Transactions on Industrial Electronics, 62(11), 7247-7255.

[17] Chong, B. V. P., & Zhang, L. (2013). Controller design for integrated PV–converter modules under partial shading conditions. Solar Energy, 92, 123-138.

[18] Boukenoui, R., Salhi, H., Bradai, R., & Mellit, A. (2016). A new intelligent MPPT method for stand-alone photovoltaic systems operating under fast transient variations of shading patterns. Solar Energy, 124, 124-142.

[19] Mutlag, A. H., Shareef, H., Mohamed, A., Hannan, M. A., & Abd Ali, J. (2014). An improved fuzzy logic controller design for PV inverters utilizing differential search optimization. International Journal of Photoenergy, 2014.

[20] Sa-ngawong, N., & Ngamroo, I. (2015). Intelligent photovoltaic farms for robust frequency stabilization in multi-area interconnected power system based on PSO-based optimal Sugeno fuzzy logic control. Renewable Energy, 74, 555-567.

[21] Palaniswamy, A. M., & Srinivasan, K. (2016). Takagi-Sugeno fuzzy approach for power optimization in standalone photovoltaic systems. Solar Energy, 139, 213-220.

[22] Dhimish, M., Holmes, V., Mehrdadi, B., & Dales, M. (2017). Diagnostic method for photovoltaic systems based on six layer detection algorithm. *Electric Power Systems Research*, *151*, 26-39.

[23] Dhimish, M., Holmes, V., Mehrdadi, B., & Dales, M. (2017). Multi-Layer Photovoltaic Fault Detection Algorithm. *High Voltage*.

[24] Yagi, Y., Kishi, H., Hagihara, R., Tanaka, T., Kozuma, S., Ishida, T., ... & Kiyama, S. (2003). Diagnostic technology and an expert system for photovoltaic systems using the learning method. Solar energy materials and solar cells, 75(3), 655-663.

[25] Chine, W., Mellit, A., Lughi, V., Malek, A., Sulligoi, G., & Pavan, A. M. (2016). A novel fault diagnosis technique for photovoltaic systems based on artificial neural networks. Renewable Energy, 90, 501-512.

[26] Mellit, A., Sağlam, S., & Kalogirou, S. A. (2013). Artificial neural network-based model for estimating the produced power of a photovoltaic module. Renewable Energy, 60, 71-78.

[27] Polo, F. A. O., Bermejo, J. F., Fernández, J. F. G., & Márquez, A. C. (2015). Failure mode prediction and energy forecasting of PV plants to assist dynamic maintenance tasks by ANN based models. Renewable Energy, 81, 227-238.

[28] Sepasi, S., Reihani, E., Howlader, A. M., Roose, L. R., & Matsuura, M. M. (2017). Very short term load forecasting of a distribution system with high PV penetration. Renewable Energy.

[29] McEvoy, A., Castaner, L., Markvart, T., 2012. Solar Cells: Materials, Manufacture and Operation. Academic Press.

[30] Sera, D., Teodorescu, R., & Rodriguez, P. (2007). PV panel model based on datasheet values. Paper presented at the 2392-2396. doi:10.1109/ISIE.2007.4374981

[31] Dhimish, M., Holmes, V., Dales, M., & Mehrdadi, B. (2017). The effect of micro cracks on photovoltaic output power: case study based on real time long term data measurements. *Micro & Nano Letters*.

[32] Dhimish, M., Holmes, V., Dales, M., Mather, P., Sibley, M., Chong, B., & Zhang, L. (2017, June). Fault detection algorithm for multiple GCPV array configurations. In *PowerTech, 2017 IEEE Manchester* (pp. 1-6). IEEE.

[33] Huang, C., Bensoussan, A., Edesess, M., & Tsui, K. L. (2016). Improvement in artificial neural network-based estimation of grid connected photovoltaic power output. Renewable Energy, 97, 838-848.

[34] Amrouche, B., & Le Pivert, X. (2014). Artificial neural network based daily local forecasting for global solar radiation. Applied energy, 130, 333-341.

[35] Cervone, G., Clemente-Harding, L., Alessandrini, S., & Delle Monache, L. (2017). Short-term photovoltaic power forecasting using Artificial Neural Networks and an Analog Ensemble. *Renewable Energy*, *108*, 274-286.

[36] Etemadi, A. (2016). Fault Detection for Photovoltaic Systems Based on Multi-resolution Signal Decomposition and Fuzzy Inference Systems. IEEE Transactions on Smart Grid.

[37] Dhimish, M., Holmes, V., Mehrdadi, B., Dales, M., & Mather, P. (2018). Photovoltaic fault detection algorithm based on theoretical curves modelling and fuzzy classification system. Energy, doi.org/10.1016/j.energy.2017.08.102.